Article

Enhanced Larvicidal Activity of New 1,2,4-Oxadiazoles against *Aedes aegypti* Mosquitos: QSAR and Docking Studies

Aluízio G. da Silva, [a] *Daniela Maria A. F. Navarro,* [*,b] *Geanne K. N. Santos,* [b]
Júlio César R. O. F. de Aguiar, [b,c] *Karla A. de França,* [b,c] *Iris Raquel M. Tébéka,* [a]
Janaína V. dos Anjos, [c] *João Bosco P. da Silva,* [*,a] *Luiz A. Kanis,* [d] *Rajendra M. Srivastava,* [c]
Ricardo Antônio W. Neves Filho [c] *and Mozart N. Ramos* [a]

*ªLaboratório de Química Teórica e Computacional, Departamento de Química Fundamental,
Universidade Federal de Pernambuco, 50740-560 Recife-PE, Brazil*

*ᵇLaboratório de Ecologia Química, Departamento de Química Fundamental,
Universidade Federal de Pernambuco, 50670-901 Recife-PE, Brazil*

*ᶜLaboratório de Síntese Orgânica, Departamento de Química Fundamental,
Universidade Federal de Pernambuco, 50670-901 Recife-PE, Brazil*

*ᵈGrupo de Pesquisa em Tecnologia Farmacêutica, Programa de Pós-Graduação em Ciências da Saúde,
Universidade do Sul de Santa Catarina, 88704-900 Tubarão-SC, Brazil*

The worldwide emergence of viral diseases such as Zika, Dengue, Chikungunya, West Nile and Yellow Fever urge the search for solutions to eliminate their common vector, the *Aedes aegypti* mosquito. This paper describes the quantitative structure-activity relationship (QSAR) and docking studies of a series of nine 3-(3-aryl-1,2,4-oxadiazol-5-yl)propionic acids (AOPA), **1-9**, previously published by our group. Additionally, three new 1,2,4-oxadiazoles, **10-12**, have also been synthesized, characterized and studied. The QSAR and docking studies of all compounds, **1-12**, clearly indicate that larger hydrophobic substituents such as biphenyl groups attached on position 3 in 1,2,4-oxadiazoles improve the larvicidal activity. It is worthwhile to mention that nanocapsulation of compounds **10-12** were necessary to help their dissolution in water and these three new 1,2,4-oxadiazoles also exhibited approximately equal or higher larvicidal activities compared to the former prototypes at stage L4.

Keywords: *Aedes aegypti*, larvicidal, 1,2,4-oxadiazole, QSAR, molecular docking

Introduction

Organic compounds as control agents against insects' pest in agriculture and human health have been intensively investigated since the Second World War.[1] The first synthetic insecticidal compound described in the literature was dichloro-diphenyl-trichloroethane (DDT). Its insecticidal effect was discovered by Müller (1939) and rapidly it became the most widely used insecticide globally, creating a new era for the use of organic compounds against insect pests.[2,3] For example, the use of DDT against *Anopheles* mosquitoes allowed a major control against malaria dissemination.[4] This compound has repellent properties too.[5] In addition, some studies using halogenated aromatic organic compounds (HAOC) like DDT were extended to parasites. This way, halogenated phenols, studied by Applegate *et al.*,[6] presented good efficiency against sea parasites like sea lamprey larvae.

More than 70 years after DDT applications were first described, new classes of HAOC, with a large spectrum of structures were developed for mosquito population control. In 1973, benzoyl-3-phenylureas showed a powerful larvicidal activity against *Aedes aegypti* (*A. aegypti*).[7] Other reports describing a variety of organic compounds active against mosquito larvae (e.g., 2-halooctadecanoic acids and alkyl 2-halooctadecanoates,[8] benzoyl-ureas and benzoyl-biurets,[9] naphthoquinones,[10] benzoheterocyclic diacylhydrazine derivatives,[11] oxime ether and oxime

esters containing benzoylphenylureas,[12] oxazolyl tetrahydropyrimido quinolinones[13] and benzoylureas with isoxazoline and isoxazole groups)[14] were published. Larvicidal compounds are useful in an integrated management control of mosquito dissemination. In order to circumvent the resistance exhibited by mosquito larvae after continued exposure to substances regularly used to control them such as temephos,[15] it is important that new compounds are continuously being synthesized and evaluated for their larvicidal activity.

In 2009, our research group synthesized 3-[3-(aryl)-1,2,4-oxadiazol-5-yl]propionic acids (AOPA) which presented good larvicidal activity against *A. aegypti* larvae, the dengue and yellow fever disease vector.[16] One of the benefits of using AOPAs is the low cytotoxicity of these compounds.[16] Our findings suggested that larvicidal activity of AOPAs is correlated to the presence of electron-withdrawing substituents on the *para* position of the phenyl ring. These results are in agreement with the quantitative structure-activity relationship (QSAR) studies of (2,6-halogenbenzoyl)-5-(4-halogen-phenyl) biuret compounds, developed by Bordas *et al*.[9] against *A. aegypti* larvae, which pointed out the presence of strong electron-withdrawing groups, like 2,6-di-fluorophenyl group as well as highly lipophilic *para*-substituents on the phenyl ring as a requisite for high larvicidal activity of the biuret derivatives.

In 2015, inspired by the co-crystallization of palmitic acid ($CH_3(CH_2)_{14}COOH$) at the *A. aegypti* Sterol Carrier Protein-2 (AeSCP-2, a proposed system related to the intracellular transport of cholesterol), we have reported a series of phenyl- and phenoxymethyl-thiosemicarbazone derivatives showing larvicidal activity against *A. aegypti* in L4 stage. Concerning these compounds, both experimental and theoretical (QSAR and docking) results strengthen the hypothesis of AeSCP-2 as a potential target for the development of new *A. aegypti* larvicidals.[17] In agreement with previous publications,[18-20] the hydrophobic character was again highlighted as an important feature of the thiosemicarbazone derivatives for improving the larvicidal activity.[17] We have also demonstrated, through nuclear magnetic resonance (NMR) experiments, that when compared to the semicarbazide moiety on the semicarbazone derivatives, the thiosemicarbazide moiety on these thiosemicarbazone derivatives has an improved capability to form hydrogen bond (H-bond) interactions with the solvent. These NMR studies coupled to density functional theory (DFT) calculation results have provided insights on the formation of H-bond interactions between the thiosemicarbazide moiety and polar amino acids of AeSCP-2.[21]

In the present work, a QSAR study on nine AOPAs previously synthesized and tested by us[16] (Scheme 1) was developed.

Scheme 1. AOPA series studied in this work.

From the QSAR analysis, three new 1,2,4-oxadiazol-5-yl propionic acids were designed and synthesized. Their larvicidal activity against *A. aegypti* was shown to be equal or higher than the former prototypes.[16] Because of the existence of both hydrophobic and hydrophilic domains in AOPAs as well as in the palmitic acid and thiosemicarbazone derivatives, docking studies for the 1,2,4-oxadiazolic compounds at AeSCP-2 were performed. From the docking calculations, a statistic analysis of the ligand-target interaction was carried out in order to improve the comprehension about the larvicidal activity at molecular level. The larvicidal bioassays performed using the compounds described in Scheme 1 were conducted using tween-80 as co-solvent. In this work, a nanoencapsulation of new biphenyl compounds was necessary due to the low solubility of the compounds in water.

Experimental

Material and methods

Molecular modelling

Density of functional theory (DFT) calculations using the hybrid functional B3LYP[22] and the basis set 6-311G(d,p) were developed using the Gaussian 09 (G09) program[23] to obtain ground state geometric, energetic, electronic and vibrational properties of the compounds under investigation **1-12**. The molecular geometry was fully optimized and the harmonic vibrational frequency calculations were both performed using the default convergence criteria of G09.

QSAR studies

In this work we have created a relationship between the response function (the larvicidal activity expressed in terms of $\log(1/LC_{50})$) and a set of molecular descriptors that our previous experience[17] as well as the literature

pointed out as important for the larvicidal activity against *Aedes aegypti*. In particular, we selected descriptors belonging to the ligand as a whole and of easy chemical interpretation, namely: (*i*) Mulliken atomic charge, (*ii*) sum of atomic charges, (*iii*) the electric dipole moment (μ), (*iv*) highest occupied molecular orbital (HOMO) energy, (*v*) lowest unoccupied molecular orbital (LUMO) energy, (*vi*) HOMO-LUMO energy difference and (*vii*) octanol-water partition coefficient (log P). In general, for QSAR studies, the data set is divided into the calibration set with which the regression model is created and the test set with which the predictions of the regression model are evaluated. Due to the relatively small number of AOPA available[16] we used compounds **1-9** (Scheme 1) to create the QSAR model through a partial least squares regression (PLSR)[24] using the leave-one-out cross-validation procedure. The PLSR was developed in a personal code written in R language[25] which it was based on the paper of Mevik and Wehrens.[26] Before the PLS calculation, the numbers used in the calibration data set (**1-9**) were autoscaled, i.e., each element on a column was subtracted by the average and divided by the standard deviation in the column. The number of latent variables was determined by the calculation of the root-mean-square error associated with the leave-one-out cross-validation procedure (RMSECV) used to create the calibration model.[27]

Docking studies of 1,2,4-oxadiazol acids in AeSCP-2

The target structure for docking calculations was taken from the Protein Data Bank[28] under the PDB code 1PZ4 for *Aedes aegypti* sterol carrier protein 2 (AeSCP-2).[29] The AeSCP-2 was treated as a rigid structure in the AutoDockTools program.[30] The ligands were also subjected to treatment in the program keeping flexible all torsion bonds and adding Gasteiger charges.[31] The program Autogrid 4.0[32] was used to generate the grid maps. After some tests, the grid dimensions $50 \times 50 \times 50$ Å with points separated by 0.375 Å were selected. The AutoDock 4.2 program[30] was used for the docking calculations. The standard docking protocol for rigid and flexible ligand docking consisted of 1000 runs *per* ligand, using an initial population of 150 individuals, with 2.5×10^6 energy evaluations, a maximum number of 27000 iterations, a mutation rate of 0.02, a crossover rate of 0.80, and an elitism value of 1. The Ligplot program,[33] using its default setting, was used to analyze the molecular interactions presented in the docking solutions.

General chemistry

All commercially available reagents were used without any further purification and the reactions were monitored by thin layer chromatography (TLC) analysis (TLC plates containing GF$_{254}$ E. Merck, Darmstadt, Germany). Melting points were determined on a Büchi apparatus (Büchi Labortechnik AG, Flawil, Switzerland) and are uncorrected. NMR spectra were recorded with a Varian Unity Plus 300 MHz spectrometer (Varian, California, USA) and referenced as following: ^{1}H (300 MHz), SiMe$_4$ as an internal standard at δ 0.00 ppm, ^{13}C (75 MHz), which dimethyl sulfoxide (DMSO-d_6, Cambridge Isotope Laboratories Inc, Andover, USA) as reference internal standard at δ 77.23 ppm. Elemental analyses were performed with a Carlo Erba instrument model E-1110 (PerkinElmer, Llantrisant, UK) and mass spectrometric analysis by direct injection on the LC/MS-IT-TOF (Shimadzu Scientific Instruments, Kyoto, Japan), all equipment in our department. 3-[3-(4-Bromophenyl)-1,2,4-oxadiazol-5-yl] propionic acid (**9**) was synthesized according to the literature procedure.[16]

Synthesis

Synthesis of AOPA derivatives **10-12**

Compound **9** (0.30 g, 1.0 mmol), suitable boronic acid (Sigma-Aldrich, Saint Louis, USA) **10-12** (1.1 mmol), K$_2$CO$_3$ (Vetec, Rio de Janeiro, Rio de Janeiro) (5 mmol), PdCl$_2$(PPh$_3$)$_2$ (Sigma-Aldrich, Saint Louis, USA) (0.02 mmol), tetrabutylammonium bromide (TBAB) (Sigma-Aldrich, Saint Louis, USA) (0.3 mmol) and H$_2$O (distilled water) (10 mL) were added in a round bottom flask (50 mL). The contents were stirred at 70 ºC for 4 h under nitrogen atmosphere. After cooling to room temperature, the reaction mixture was acidified with 10% v/v HCl (Vetec, Rio de Janeiro, Rio de Janeiro) solution and extracted with ethyl acetate (Química Moderna, Barueri, São Paulo) (3×20 mL). The organic phase was dried over anhydrous MgSO$_4$ (Vetec, Rio de Janeiro, Rio de Janeiro) and filtered through a celite pad (Merck, Billerica, USA). The solvent was removed under reduced pressure and the crude material was crystallized and re-crystallized from chloroform to give the pure products **10-12**.

3-(3-Biphenyl-4-yl-1,2,4-oxadiazol-5-yl)-propionic acid (**10**)

Colorless crystals; yield: 43%; mp 197-198 ºC; ^{1}H NMR (300 MHz, DMSO-d_6) δ 2.87 (t, 2H, *J* 6.9 Hz, CH$_2$), 3.21 (t, 2H, *J* 6.9 Hz, CH$_2$), 7.41-7.53 (m, 3H, H$_{arom}$), 7.74 (d, 2H, *J* 8.4 Hz, H$_{arom}$), 7.86 (d, 2H, *J* 8.4 Hz, H$_{arom}$), 8.07 (d, 2H, *J* 8.4, 1.2 Hz, H$_{arom}$), 12.5 (s, 1H, OH); ^{13}C NMR (75 MHz, DMSO-d_6) δ 21.7, 29.8, 125.1, 126.8, 127.4, 127.5, 128.1, 129.0, 138.9, 142.9, 167.1, 172.8, 179.7; anal. calcd. for C$_{17}$H$_{14}$N$_2$O$_3$ (C,H,N): C 69.31%, H 4.75%, N 9.51%; found: C 69.56%, H 4.37%, N 9.42%.

3-[3-(4'-Methyl-biphenyl-4-yl)-[1,2,4]oxadiazol-5-yl]-propionic acid (11)

Colorless crystals; yield: 52%; mp 208-209 °C; ^{1}H NMR (300 MHz, DMSO-d_6) δ 2.35 (s, 3H, CH$_3$), 2.87 (t, 2H, J 6.9 Hz, CH$_2$), 3.22 (t, 2H, J 6.6 Hz, CH$_2$), 7.30 (d, 2H, J 8.4 Hz, H$_{arom}$), 7.63 (d, 2H, J 8.1 Hz, H$_{arom}$), 7.83 (d, 2H, J 8.7 Hz, H$_{arom}$), 8.05 (d, 2H, J 8.7 Hz, H$_{arom}$), 12.5 (s, 1H, OH); ^{13}C NMR (75 MHz, DMSO-d_6) δ 20.7, 21.7, 29.9, 124.8, 126.6, 127.0, 127.5, 129.6, 136.0, 137.6, 142.8, 167.2, 172.8, 179.6; HRESIMS *m/z*: 307.0748 [M − H]⁻.

3-[3-(4'-Chloro-biphenyl-4-yl)-1,2,4-oxadiazol-5-yl]-propionic acid (12)

Colorless crystals; yield: 53%; mp 206-207 °C; ^{1}H NMR (300 MHz, DMSO-d_6) δ 2.86 (t, 2H, J 6.9 Hz, CH$_2$), 3.21 (t, 2H, J 6.9 Hz, CH$_2$), 7.54 (d, 2H, J 8.7 Hz, H$_{arom}$), 7.75 (d, 2H, J 8.7 Hz, H$_{arom}$), 7.84 (d, 2H, J 8.7 Hz, H$_{arom}$), 8.06 (d, 2H, J 8.4 Hz, H$_{arom}$), 12.5 (s, 1H, OH); ^{13}C NMR (75 MHz, DMSO-d_6) δ 21.7, 29.8, 125.4, 127.3, 127.6, 128.5, 129.0, 133.0, 137.7, 141.5, 167.1, 172.8, 179.7; HRESIMS *m/z*: 327.0161 [M − H]⁻.

Preparation of solutions and nano-capsules used in the larvicidal bioassay

Nano-capsule preparation of biphenyl 1,2,4-oxadiazoles: (*i*) oil phase: the compounds were weighed on an analytical balance. Chlorine biphenyl 1,2,4-oxadiazole **12** (2 mg) and 5 mg of *p*-methyl biphenyl 1,2,4-oxadiazole and biphenyl 1,2,4-oxadiazole **10** were used for the preparation of nanocapsules. Each compound was mixed with 100 mg of cellulose acetate (Sigma-Aldrich, Saint Louis, USA), 50 mg of polyethylene glycol polyethylene distearate (Sigma-Aldrich, Saint Louis, USA) and 75 mg of sunflower oil. This mixture was solubilized in 25 mL of acetone (Química Moderna, Barueri, Brazil) and 2 mL of ethyl acetate. (*ii*) Water phase: 75 mg of tween 80 (Sigma-Aldrich, São Paulo, Brazil) were solubilized in 53 mL of highly purified water (pH 6.5-7.0). The oil phase was injected in the water phase (20 mL) by minute under stirring (150 rpm). The mixture was stirred for 10 min, then the solvents were evaporated under reduced pressure at 35 °C. The solution obtained was used to prepare the diluted solutions in deionized water. Control solution was prepared under the same conditions but without the compounds under investigation. Encapsulation average data was 70% (65-76) of 1,2,4-oxadiazoles (**10**), 55% (45-64) (**11**) and 66% (61-69) (**12**), respectively.

Larvicidal bioassay

The larvicidal activity of the biphenyl-1,2,4-oxadiazoles (**10-12**) was evaluated using an adaptation of the method recommended by the World Health Organization.[34-37] Stock solutions were prepared by dissolving 5 mg of the compounds in either ethanol (Dinâmica, Indaiatuba, Brazil) or tween-80 (Sigma-Aldrich, São Paulo, Brazil) and then diluting it with 50 mL of distilled water. Dilution of the stock solutions allowed the preparation of the adequate concentrations to be tested. Fourth instar *A. aegypti* were added to a beaker (20 larvae) containing these adequate solutions. Four replicate assays were carried out for every sample concentration, and for each assay a negative control was included and prepared as described without the active compounds. Mortality of the larvae was determined after 48 h of incubation at 28 ± 2 °C, 70 ± 10% with relative humidity. Larvae were considered dead when they did not respond to stimulus or did not rise to the surface of the solution. The lethal concentration values lethal concentration which kill 10% (LC$_{10}$) and lethal concentration which kill 50% (LC$_{50}$) were calculated by probit analysis using StatusPlus2006 software.[38]

Results and Discussion

Before starting the discussion of the results, an important aspect to highlight is that, although Figure 1 and Tables 1 and 2 show results for twelve compounds, the regression model was developed only for the compounds **1-9** (see Experimental section). Based on the regression results obtained for these nine compounds, then we move on to the next steps of the research namely: the design, the synthesis and the test of larvicidal activity.

Since most of the descriptors were obtained from DFT calculations, it is important to know about the geometry of these compounds. In Figure 1, the B3LYP/6-311G(d,p) optimized structures (for details see Supplementary Information (SI) section) and the first infrared vibration mode for compounds **1**-**12** are shown.

As one can see, the infrared calculations indicate that all structures represent local minima in the potential energy surface. We have used these optimized geometries (see SI section) to access the electronic parameters used for creating the QSAR model.

QSAR model

Table 1 depicts the data matrix used to develop the QSAR model (**1-9**) and for the three new AOPAs (**10-12**).

An important aspect to be taken into account in developing a PLS model is the number of latent variables to be included in the model.[27] Figure 2 shows the RMSECV value as a function of the number of latent variables (NLV) included in the calibration model (**1-9**).
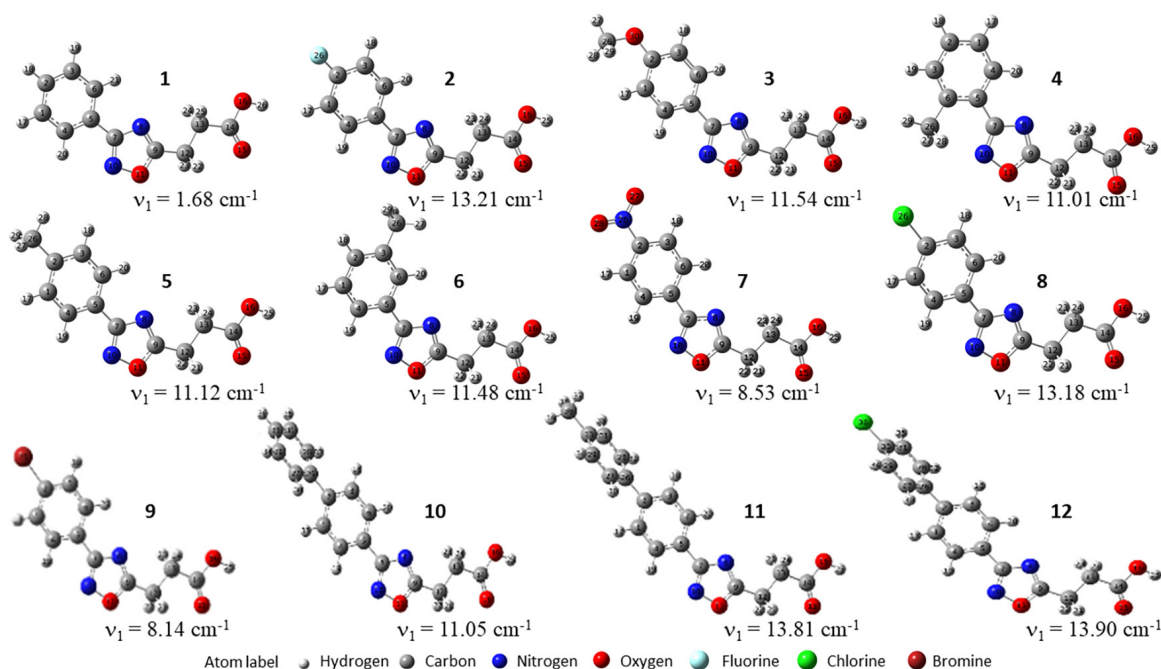
Figure 1. B3LYP/6-311G(d,p) optimized structures and the lowest infrared vibrational frequency mode for the compounds **1-12**.

Table 1. Experimental *A. aegypti*'s L4 larvicidal activity, electronic and steric descriptors calculated at B3LYP/6-311G(d,p) level of theory and hydrophobic descriptors of AOPA derivatives

Numbering	pLC$_{50}$[a]	μ / D	ε$_{HOMO}$ / eV	ε$_{LUMO}$ / eV	Δε[d] / eV	qC3 / e	qC6 / e	qN2 / e	qN4 / e	qO1 / e	Σq$_{benz}$[d] / e	Σq$_{ring}$[e] / e	logP
1	3.3439[b]	2.598	−6.874	−1.506	5.368	0.259	−0.190	−0.142	−0.365	−0.224	−0.501	−0.133	1.78
2	3.4637[b]	2.445	−6.859	−1.562	5.297	0.263	−0.205	−0.144	−0.367	−0.222	−0.225	−0.130	1.98
3	3.5406[b]	2.418	−6.184	−1.265	4.919	0.261	−0.205	−0.150	−0.368	−0.226	−0.282	−0.144	1.86
4	3.5153[b]	2.232	−6.762	−1.412	5.350	0.255	−0.164	−0.156	−0.372	−0.226	−0.488	−0.161	2.33
5	3.5478[b]	2.834	−6.627	−1.404	5.224	0.257	−0.187	−0.144	−0.366	−0.225	−0.472	−0.139	2.33
6	3.5611	2.988	−6.725	−1.440	5.284	0.257	−0.185	−0.142	−0.366	−0.224	−0.474	−0.136	2.33
7	3.7169[b]	4.868	−7.610	−2.938	4.672	0.266	−0.179	−0.134	−0.364	−0.216	−0.190	−0.107	1.60
8	3.9539[b]	2.624	−6.900	−1.754	5.146	0.263	−0.194	−0.141	−0.366	−0.221	−0.414	−0.125	2.42
9	4.2907[b]	2.561	−6.821	−1.761	5.060	0.263	−0.192	−0.141	−0.366	−0.221	−0.446	−0.125	2.67
10	4.2573[c]	2.713	−6.370	−1.696	4.674	0.255	−0.181	−0.143	−0.365	−0.224	−0.411	−0.137	3.54
11	4.8729[c]	3.058	−6.212	−1.642	4.570	0.255	−0.181	−0.143	−0.365	−0.224	−0.342	−0.137	4.09
12	5.1249[c]	2.556	−6.465	−1.862	4.603	0.256	−0.181	−0.142	−0.365	−0.222	−0.408	−0.133	4.19

[a]For statistics parameters see Table S1 in the Supplementary Information section; [b]reference 16; [c]this work; [d]energy difference between the HOMO and LUMO orbitals; [d]carbon Mulliken charge sum over the phenyl ring; [e]total Mulliken charge on the 1,2,4-oxadiazole ring. LC$_{50}$: lethal concentration which kill 50%; μ: electric dipole moment ; logP: octanol-water partition coefficient.

As one can see in the Figure 2, four latent variables minimize the RMSECV for the calibration set. Considering four latent variables, it is possible to describe 85.57 and 98.12% of the information in the X (descriptors) and Y (log(1/LC$_{50}$)) matrixes, respectively.

The regression equation between the larvicidal activity and the molecular descriptors for compounds **1-9** is given in the equation 1:

$$\log(1/LC_{50}) = 3.6593 - 0.0577.\mu + 0.0322.E_{HOMO} - 0.0421.E_{LUMO} - 0.1438.DeltaE + 0.1132.qC_3 + 0.0163.qC_6 + 0.0005.qN_2 - 0.0277.qN_4 + 0.0659.qO_1 - 0.0885.\Sigma q_{benz} + 0.0413.\Sigma q_{ring} + 0.2162.\log P \quad (1)$$

Using the autoscaled descriptor data in equation 1, one can calculate the predicted larvicidal activity, which the values are given in Table 2. Here it is very important to remember that the average and the standard deviation used to autoscale the data are those obtained for the calibration data set (**1-9**).

The information contained in Table 2 can be alternatively visualized in Figure 3a, which shows the experimental log(1/LC$_{50}$) *versus* the predicted log(1/LC$_{50}$) activities for the calibration set. The adjustment of the PLS model can be appreciated by the corresponding residue plot as shown in Figure 3b.

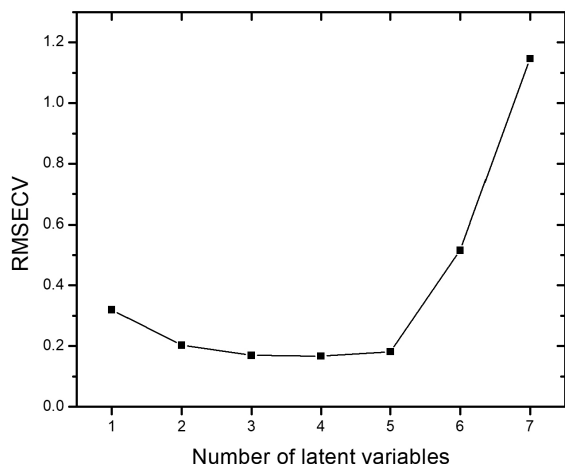Table 2 and Figure 3a point out a good agreement

Figure 2. RMSECV plot for the calibration model (compounds **1-9**) as a function of the number of latent variables used in the PLS regression.

between predicted and observed activities for the calibration set. The quality of the regression may also be appreciated by the high statistic parameter R^2 (calibration set) $= 0.9812$, as well as the random distribution of the points around zero in the residue plot (Figure 3b).

In Figure 4 the score and loading plots obtained from the PLS model (based on the data set presented in Table 1 for compounds **1-9**) are shown for the first two latent variables.

From Table 2 and Figure 4a one can note two series of compounds with increasing larvicidal activity, they are: (**4**, **5**, **6**, **7**) and (**1**, **2**, **5**, **6**, **8**, **9**). On the other hand, Figure 4b shows that the first latent variable, with 54.1% of the variance, it is dominated by electronic descriptors like atomic or sum of atomic charges, the dipole moment

and HOMO/LUMO orbital energies, whereas, the second latent variable, with 15.7% of the variance, is dominated mainly by the hydrophobic descriptor, logP.

Therefore, these results indicate that there are two ways to improve the larvicidal activity: by increasing its polar and/or its lipophilic character. A reconciliation to this apparent paradox result will be explained by the molecular docking study results in the next sub-section.

Taking the series (**1**, **2**, **5**, **6**, **8**, **9**) as reference, hydrophobic substituents which boost the parameter logP are expected to improve the larvicidal activity. In fact, the importance of the parameter logP can also be appreciated by its larger coefficient in the QSAR equation 1. In order to verify this hypothesis, three new compounds (Figure 1) were designed **10-12** (Scheme 2), synthesized and their larvicidal activities evaluated (Table 2).

Synthesis of the new compounds

The synthesis of target compounds **10-12** was carried out through a palladium catalyzed Suzuki cross-coupling reaction between the carboxylic **9** and boronic acids. Albeit the existence of several protocols for the Suzuki reaction, the method described by Zhang and co-workers[39] was employed, because it tolerates the presence of an unprotected carboxylic acid functionality and uses water as solvent (Scheme 2).

The reaction worked well and gave the desired products in 43-53% yields after conventional work up and re-crystallization. The structures of the synthesized compounds

Table 2. Experimental L4 and predicted *A. aegypti*'s larvicidal activities of AOPAs

Numbering	Substituent	LC_{50} (exp.)[a] / (mmol L^{-1})	LC_{50} (pred.)[b] / (mmol L^{-1})	log (1/LC_{50}) (exp.)	log (1/LC_{50}) (pred.)
1	H	453.0[c]	515.3	3.3439[c]	3.2879
2	*p*-F	343.8[c]	354.9	3.4637[c]	3.4499
3	*p*-CH$_3$O	288.0[c]	303.3	3.5406[c]	3.5182
4	*o*-CH$_3$	305.3[c]	295.7	3.5153[c]	3.5292
5	*p*-CH$_3$	283.3[c]	247.4	3.5478[c]	3.6066
6	*m*-CH$_3$	274.7[c]	259.7	3.5611[c]	3.5855
7	*p*-NO$_2$	191.9[c]	184.2	3.7169[c]	3.7347
8	*p*-Cl	111.2[c]	102.7	3.9539[c]	3.9884
9	*p*-Br	51.2[c]	58.4	4.2907[c]	4.2336
				RMSEC	0.0378
				RMSECV	0.1674
				R^{2}cal	0.9812
10	Ph-	55.3[d]	21.7	4.2573[d]	4.6643
11	*p*-CH$_3$-Ph-	13.4[d]	10.0	4.8729[d]	5.0008
12	*p*-Cl-Ph-	7.5[d]	6.2	5.1249[d]	5.2061
				RMSE (**10-12**)	0.2508
				R^2 (**10-12**)	0.9903

[a]For statistics parameters see Table S1 in the Supplementary Information section; [b]PLS prediction; [c]reference 16; [d]this work. LC_{50}: lethal concentration which kill 50%; R^2: coefficient of determination; RMSECV: root-mean-square error associated with the leave-one-out cross-validation procedure; R^{2}cal: coefficient of determination for the calibration set.
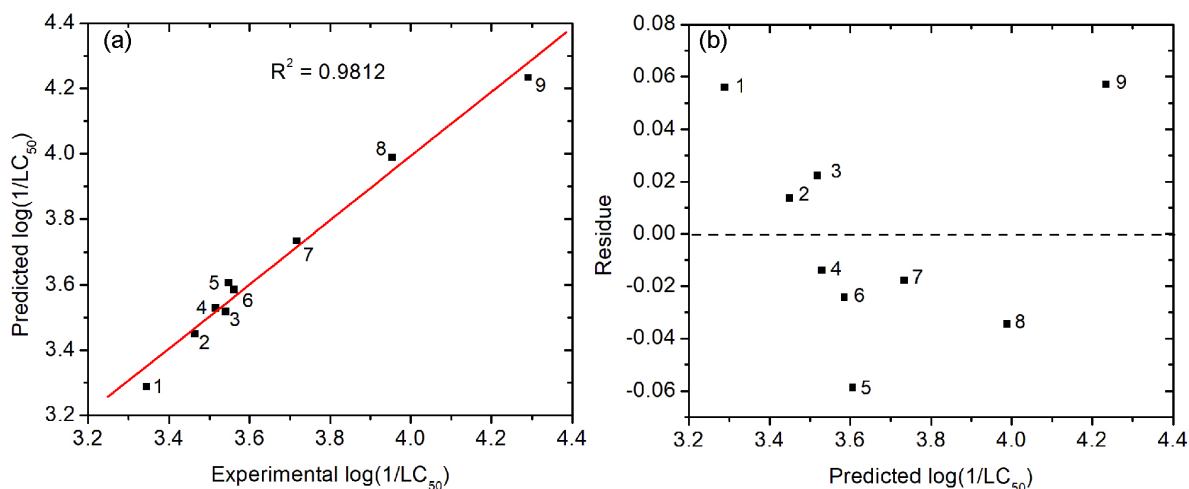
Figure 3. QSAR graphics for AOPA derivatives **1-9**: (a) predicted *versus* experimental activities and (b) residual predicted activity.
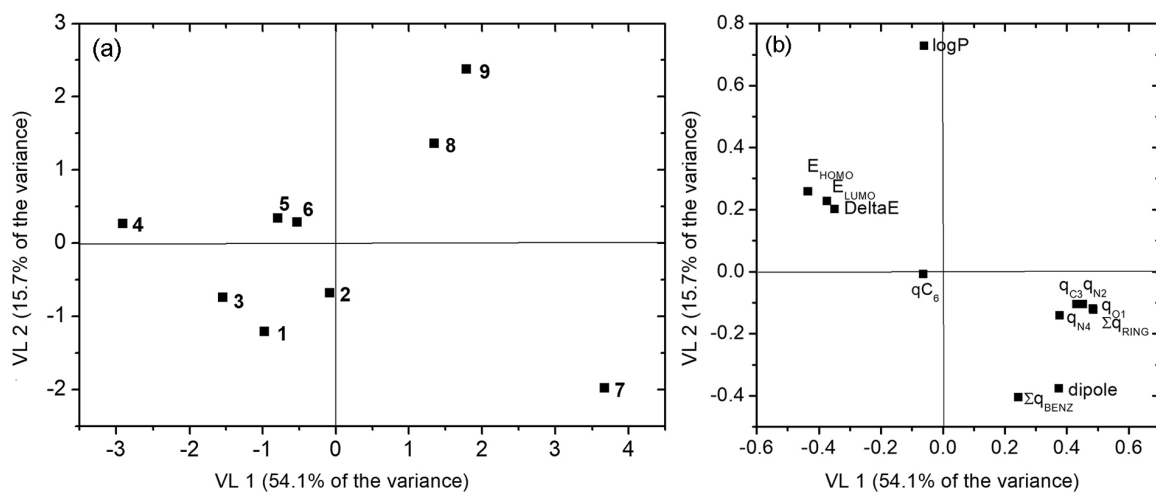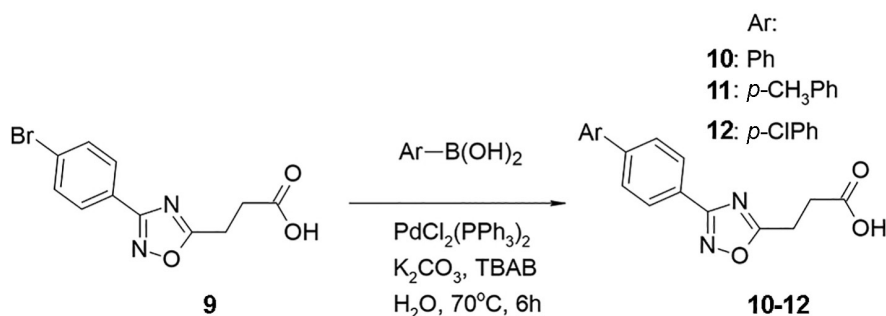

Figure 4. PLS analysis for the calibration set: (a) scores and (b) loadings plot.

Scheme 2. Reaction leading to the formation of biphenyl-1,2,4-oxadiazoles

were confirmed by ^{1}H, ^{13}C NMR spectra and high-resolution mass spectrometry (HRMS) or elemental analyses.

Larvicidal activity and QSAR prediction for **10-12**

The calculated descriptors and the experimental larvicidal activities for the compounds **10-12** are presented in the last three entries in Tables 1 and 2.

Some aspects from Table 1 must be stressed here. Since the calculated parameter logP for compounds **1-9** ranged from 1.60 to 2.67, whereas for 1,2,4-oxadiazoles **10-12** it ranges from 3.54 to 4.09, it is not surprising to observe a limited water solubility for these three last compounds. In order to overcome this solubility problem, nanocapsules containing **10-12** were prepared (see Experimental section) and their larvicidal activities were evaluated (Table 2).

The new nanoencapsulated products **10-12** are very active (Tables 1 and 2).

While the activity for **10** (LC$_{50}$ = 55.3 mmol L^{-1}) is similar to **9** (LC$_{50}$ = 51.2 mmol L^{-1}), the activities of **11** (LC$_{50}$ = 13.4 mmol L^{-1}) and **12** (LC$_{50}$ = 7.5 mmol L^{-1}) indicate an important improvement in the larvicidal activity. Just for comparison, the LC$_{50}$ for the most active thiosemicarbazone derivative was 20.9 mmol L^{-1}.[17]

It may be observed from Table 2 that the presence of a halogen substituent like chlorine at *para* position (**12**) improves the activity. The importance of electron-withdrawing substituents attached to a phenyl ring in compounds with larvicidal activity against *A. aegypti* was previously reported.[10,15] In 2014, Scotti *et al.*[40] stressed the importance of hydrophobicity to explain the potency variance of fifty-five active compounds against *A. aegypti* larvae using chemometric analysis.

Docking

Palmitic acid (CH$_3$(CH$_2$)$_{14}$COOH) was used as the model system to check the reliability of the docking calculations for our compounds at AeSCP-2. After confirming the re-docking of palmitic acid at AeSCP-2 (binding energy 8.32 kcal mol^{-1}), the docking calculations of palmitic acid at this target were developed for one thousand poses. The overlap of twenty random conformers of palmitic acid at AeSCP-2 is presented in the Figure S13 of SI section. In Figure 5a the binding energy distribution is shown. The average binding energy 7.78 kcal mol^{-1} is lower than the average values to **10-12**, as this will be seen soon. Because palmitic acid has a long methylenic tail a larger number of AeSCP-2's hydrophobic residues can be accessed (Figure 5b). In 2003, Lan and co-workers,[29] based on the X-ray data of palmitic acid at AeSCP-2 point out sixteen residues that can have hydrophobic interaction to palmitic

acid.[29] Thirteen of them have been achieved (Figure 5b) in the conformational search presented in this work.

Figures 6 and 7 show the docking results for compounds **1** and **10** as representative systems for the set of compounds (**1-6**, **8**, **9**) and (**10-12**), respectively. Because the docking prediction for **7** is quite different from other compounds (see Figure S7 of SI section), it was considered an outlier and was therefore not included in the analysis below. The full set of binding energy distribution for the reminder compounds is given in the SI section.

Figure 6a shows that **1** exhibits a bimodal binding energy distribution at AeSCP-2. A close inspection of each mode reveals two different ways of binding of compound **1** at AeSCP-2. These have been termed as linear (Figure 6d) and curved (Figure 6e) structures for the conformers related to the lower (Figure 6b) and higher (Figure 6c) binding energy of oxadiazole **1** at AeSCP-2, respectively. In both conformers, the experimental structure of palmitic acid[29] is included for comparison. It is possible to observe that the curved structures of **1** exhibit a larger range of binding energies (from 8.8 to 9.8 kcal mol^{-1}) compared to the linear structures (8.5 to 8.9 kcal mol^{-1}). It is probably associated to the flexibility of the methylenic moiety which allows the carboxylate group to rotate and explore a larger number of polar residues in AeSCP-2. On the other hand, the linear structures seem to be more overlapped and more buried into the hydrophobic pocket than the curved structures. Such statement can be appreciated by the largest overlap between the linear structures and the structure of palmitic acid (Figure 6d). These molecular docking results suggest that there are two opportunities for the binding of compound **1**, i.e., on the hydrophilic and on the hydrophobic domains of AeSCP-2. Therefore, when the hydrophobicity of these compounds is improved by, for instance, introducing a second phenyl group like in **10-12** (Table 1), it is nice to observe from the conformational search of **10** that only a
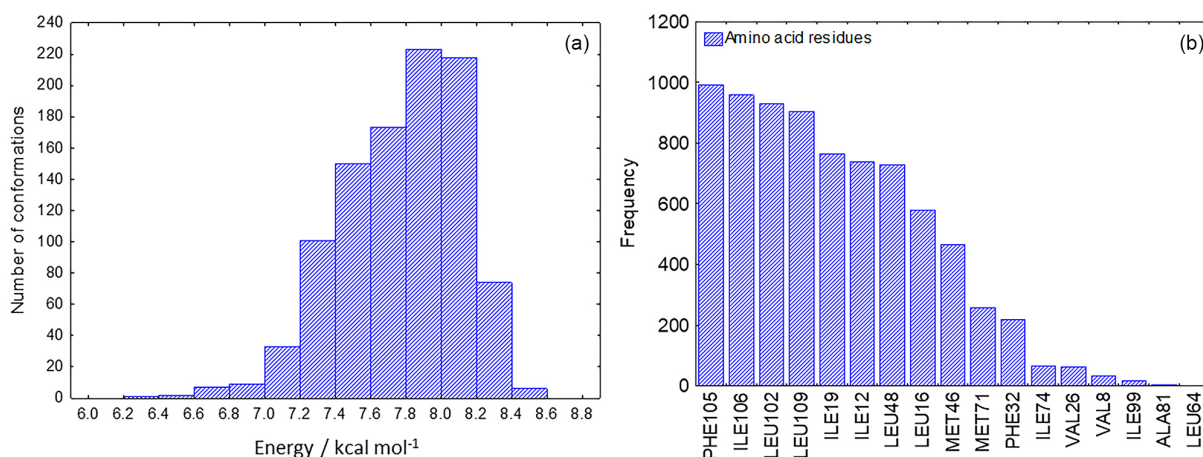

Figure 5. Palmitic acid at AeSCP-2: (a) binding energy distribution and (b) frequency of hydrophobic residues of AeSCP-2 interacting to palmitic acid.
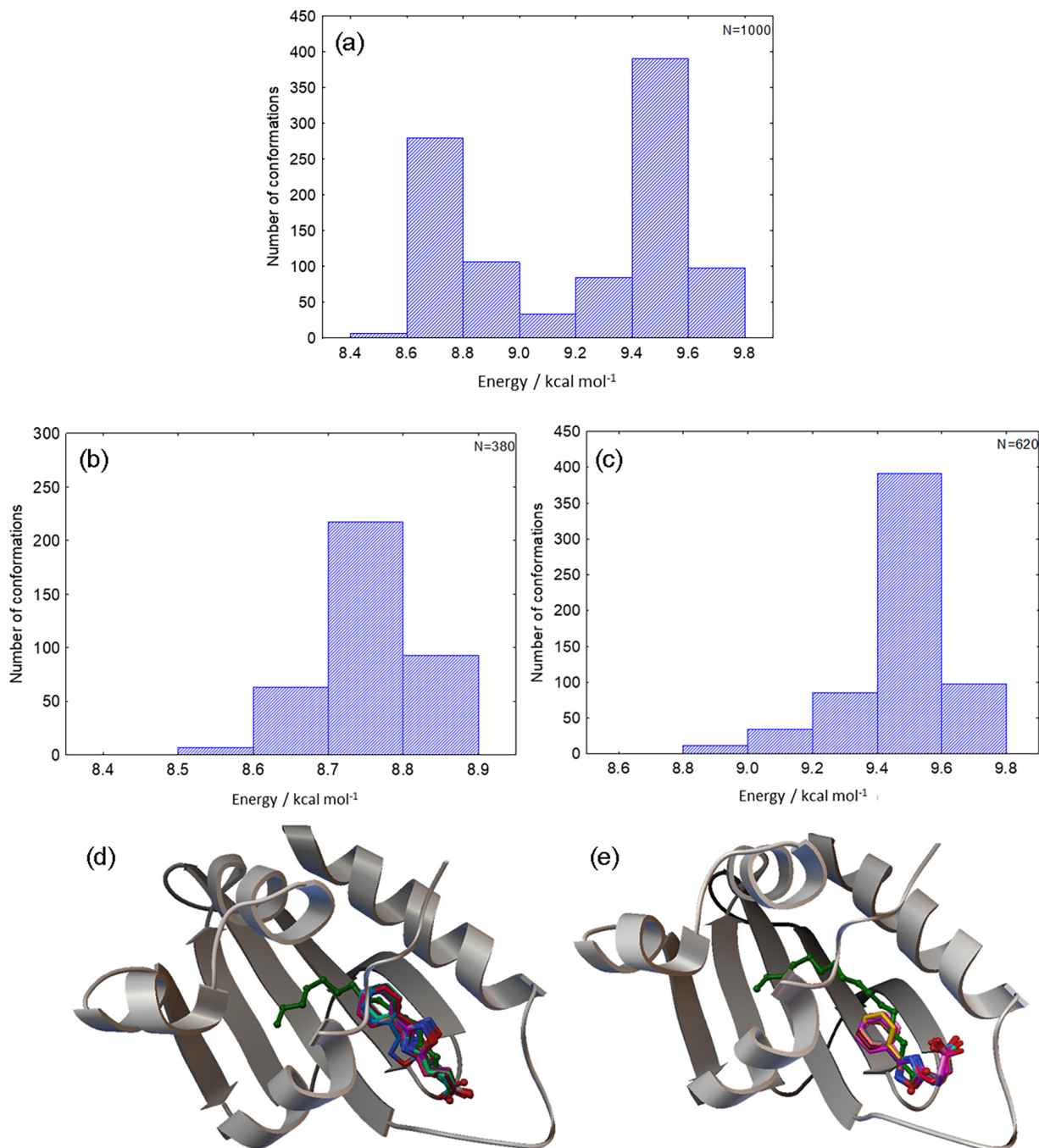
Figure 6. Docking of **1** at AeSCP-2: (a) bimodal binding energy distribution, (b-c) individual distributions related to (a), (d) overlap of twenty random structures related to the distribution in (b) and (e) overlap of twenty random structures related to the distribution in (c). The structure of palmitic acid $(CH_3(CH_2)_{14}COOH)$ was obtained from PDB (1PZ4).

unimodal and higher binding energy distribution appears (Figure 7a). The effect of better exploring the hydrophobic pocket of AeSCP-2 by **10** can be appreciated by the superposition of the overlapped conformers and the palmitic acid structures (Figure 7b). Another way to appreciate the exploration of the hydrophobic pocket of AeSCP-2 by our compounds is through the frequency analysis of hydrophobic residues interaction. Figures 8a and 8b show

the histograms of AeSCP-2's hydrophobic residues that make interaction to compounds **1** and **10**, respectively.

Considering the hydropathy scale,[41] the amino acids would have the following order of hydrophobicity: Ile > Val > Leu > Phe > Cys > Met > Ala. Therefore, from the comparison of Figures 6a and 6b, some aspects must be pointed out. First, **10** can probe a larger number of hydrophobic residues than **1**. Second, among the
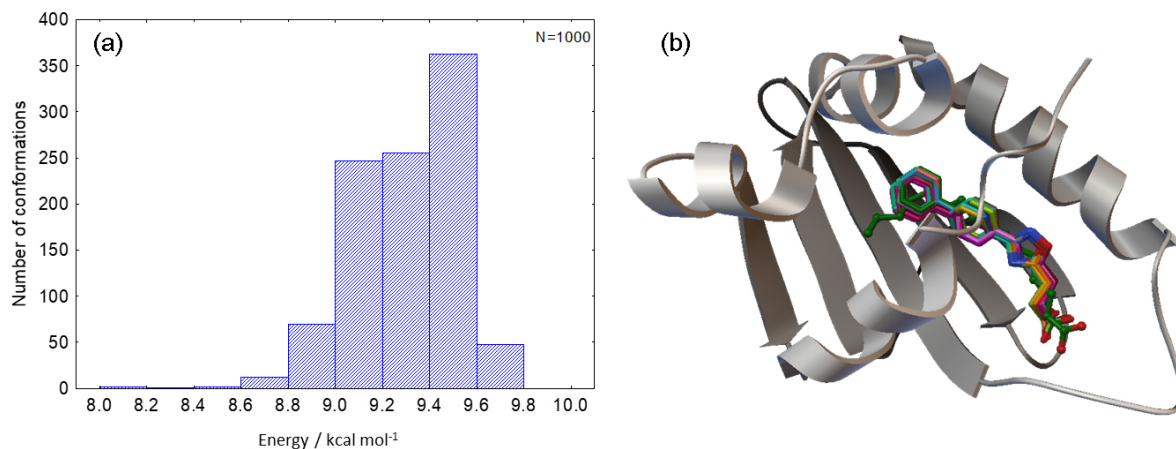
Figure 7. Docking of **10** in AeSCP-2: (a) unimodal binding energy distribution, (b) overlap of twenty random structures related to the distribution in (a). The structure of palmitic acid ($CH_3(CH_2)_{14}COOH$) was obtained from PDB (1PZ4).
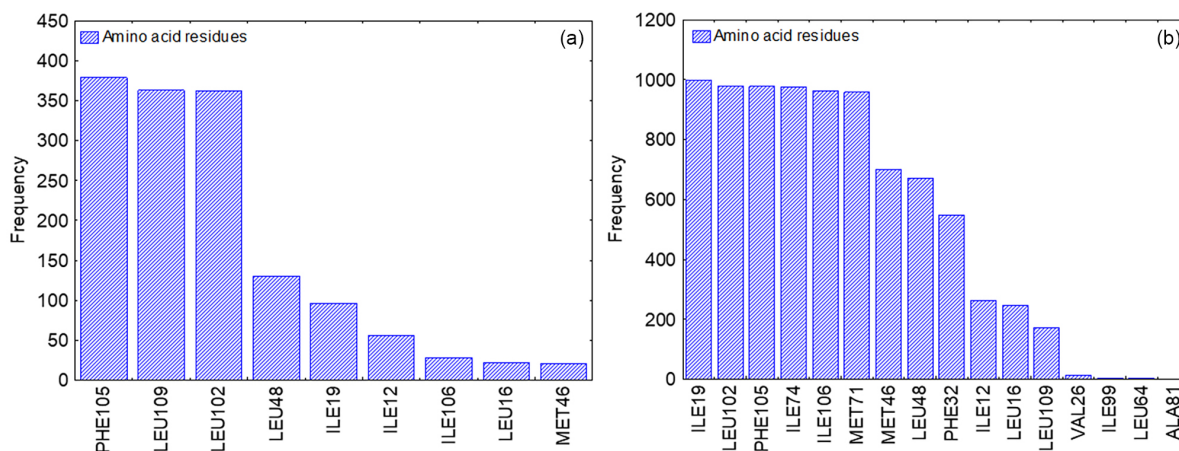

Figure 8. Histogram of hydrophobic residues of AeSCP-2 interacting to: (a) **1** and (b) **10**.

most frequent residues for **1** there are three residues of intermediate hydropathy score (Phe105, Leu102 and Leu109) whereas for **10** there are three residues of high (Ile19, Ile74 and Ile106) and three residues of intermediate hydropathy score (Phe105, Leu102 and Leu48). In particular, it is worth noting that in one thousand poses the residue Ile106 appears only 28 times for **1** whereas it is found 962 times for **10**. In Figure 9 the intermolecular interactions associated to the lowest energy pose of **10-12** with amino acid residues at AeSCP-2 are shown.

Figure 9 confirms that many amino acid residues of AeSCP-2 interacting with the five and six member rings of **10-12** are between those presented in Figure 8b.

The importance of hydrophobic interactions between isoleucine and aromatic rings in biological systems has been previously reported in the literature. For instance, the hydrophobic interaction between isoleucine and the thiazolidinic and pyrimidinic rings has been associated to the reactive V shape conformation of thiamine diphosphate-requiring enzymes.[42] Another example is the importance

of isoleucine for the hydrophobic interaction between the self-associated α and β binding sites of spectrin.[43] Third, the residues Phe105 and Leu102 interact to both **1** and **10** because they make a π-stack interaction to the 1,2,4-oxadiazol ring and hydrophobic interaction to the phenyl group, respectively (Figure 10). In fact, the ability of leucine to make a hydrophobic interaction with the oxadiazole moiety was previously described in the literature.[44] The low frequency residues Ile99 and Val26 in **10** point out for new opportunities of chemical modification that are now being tested in our group.

In the SI section it is possible to check that the histogram of frequency for the hydrophobic residues of AeSCP-2 interacting with other sets of 1,2,4-oxadiazol acid derivatives (**2-6**, **8**, **9**) and (**11**, **12**) also behavior like that to **1** and **10**, respectively.

The variation of the experimental larvicidal activity data (expressed in terms of (log (1/LC_{50})) using data from Tables 1 and 2) against the docking score may be appreciated in Figure 11.
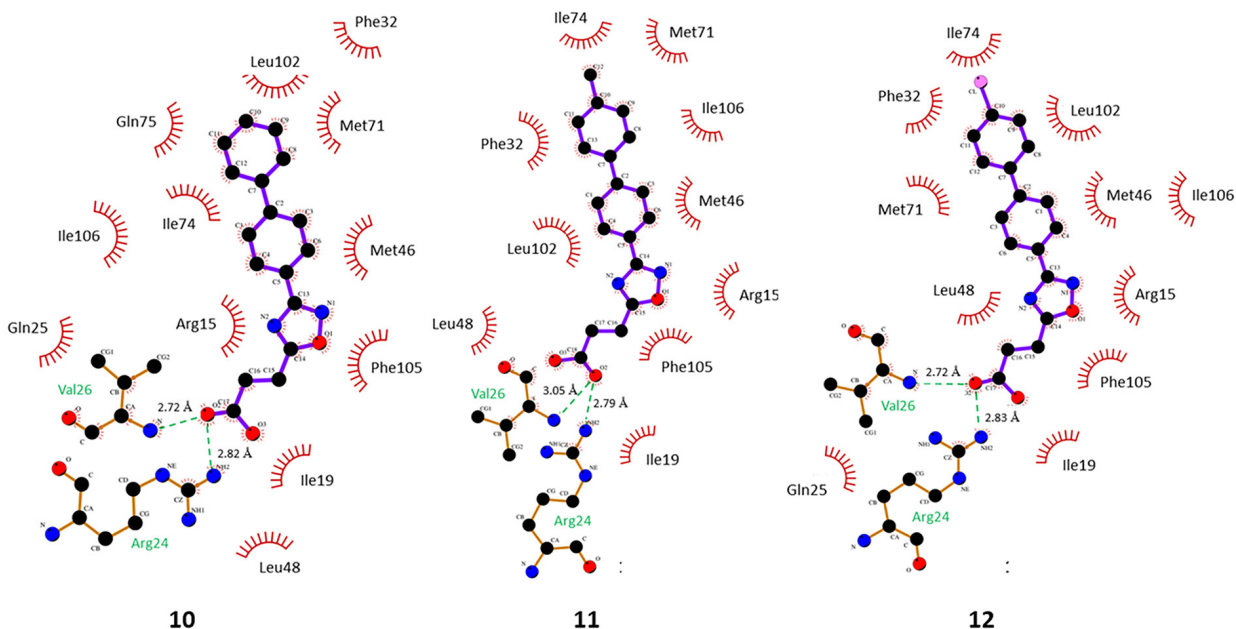
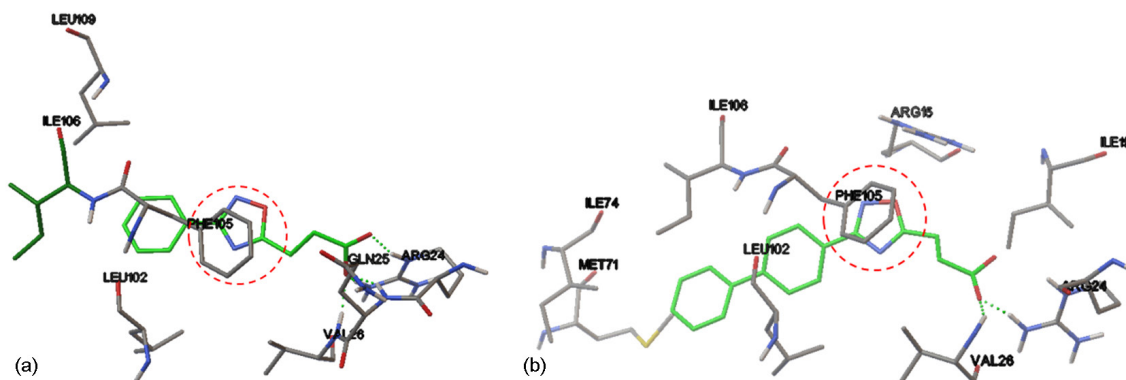**Figure 9.** Principal hydrophobic and polar intermolecular interactions of the amino acid residues of AeSCP-2 with **10-12**.

Figure 10. π-Stack interaction between AeSCP-2's residue Phe105 and the 1,2,4-oxadiazol ring (red dashed circle) of: (a) **1** and (b) **10**.

Although in Figure 11, the larvicidal activity represents the capacity the molecules to kill the whole larvae whereas
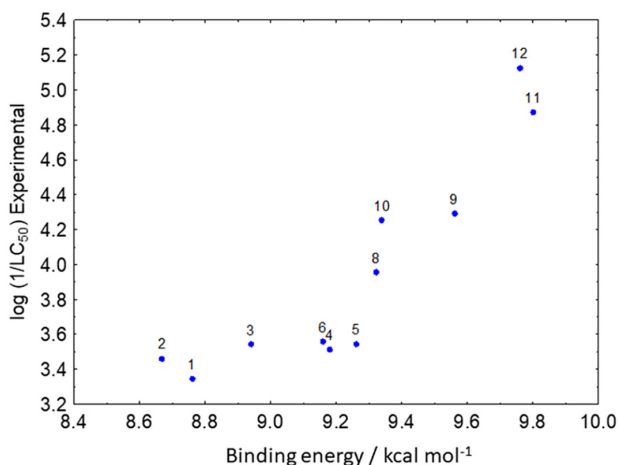

Figure 11. Comparison between experimental larvicidal activity *versus* the docking score of AOPA derivatives in AeSCP-2.

the binding energy is related to a specific target (AeSCP-2), it is notable that the most active compounds are in general associated to the larger binding energies.

Conclusions

Quantitative structure activity relationship (QSAR) studies of already synthesized AOPAs substituted at *ortho*, *meta* and *para* positions of the aryl ring led us to a better understanding of the role of the hydrophobic descriptor for the *Aedes aegypti* larvicidal activity in the L4 stage.

Taking this into account, three new AOPA derivatives were predicted, synthesized and their larvicidal activities evaluated. The QSAR prediction of improved larvicidal activities for the new compounds was observed. The molecular docking results corroborate the interaction of the hydrophobic moieties of these new AOPA compounds with hydrophobic residues at AeSCP-2.

It highlights that a theoretically oriented chemical modification (in this case the introduction of the second phenyl ring) represents a rational design strategy for exploring opportunities of intermolecular hydrophobic interaction offered by the biomolecular target AeSCP-2. In this sense, it is interesting to observe that, recently, Singarapu *et al.*[45] using solution NMR experiments showed that Sterol Carrier Protein 2 Like 2 (SCP2L2) can interact to palmitate through the hydrophobic residues Ile, Val, Leu, Met and Ala. Therefore, these results shed lights on the possibility that 1,2,4-oxadiazol acid derivatives presented in this work may also interact to this isoform of AeSCP2.

Supplementary Information

Supplementary data is available free of charge at http://jbcs.sbq.org.br as PDF file.

Acknowledgments

Author Contributions

A. G. da Silva, Mozart N. Ramos and I. R. M. Tébéka developed the quantum chemistry and docking calculations. J. B. P. da Silva and D. M. A. F. Navarro participated interpreting the results and writing the manuscript. G. K. N. Santos, J. C. R. O. F. de Aguiar, K. A. de França developed the larvicidal bioassays, J. V. dos Anjos, R. M. Srivastava and R. A. W. Neves Filho synthesized the AOPA. Luiz A. Kanis prepared the nano-capsules.

References

1. Loffler, E. S.; Hoskins, W. M.; *J. Econ. Entomol.* **1946**, *39*, 589. [Crossref]

2. Tuzimski, T. In *Encyclopedia of Analytical Science*, 3ʳᵈ ed.; Elsevier: Amsterdam, 2019, p. 391-398. [Crossref]

3. Huckett, H. C.; *J. Econ. Entomol.* **1946**, *39*, 184 [Crossref]; Hocking, K. S.; *Trans. R. Soc. Trop. Med. Hyg.* **1947**, *40*, 589. [Crossref]

4. Abate, A.; Hadis, M.; *Trop. Med. Int. Health* **2011**, *16*, 486. [Crossref]

5. Opar, A.; *Nat. Med.* **2007**, *13*, 1002. [Crossref]

6. Applegate, V. C.; Howell, J. H.; Smith, M. A.; *Science* **1958**, *127*, 336. [Crossref]

7. Wellinga, K.; Mulder, R.; van Daalen, J. J.; *J. Agric. Food Chem.* **1973**, *21*, 993. [Crossref]

8. Hwang, Y.-S.; Navvab-Gojrati, H. A.; Mulla, M. S.; *J. Agric. Food Chem.* **1978**, *26*, 1293. [Crossref]

9. Bordas, B.; DeMilo, A. B.; Lopata, A.; Haught, S. B.; *Tag.-Ber., Akad. Landwirtsch.-Wiss.* **1989**, *274*, S157.

10. Ribeiro, K. A. L.; de Carvalho, C. M.; Molina, M. T.; Lima, E. P.; López-Montero, E.; Reys, J. R. M.; de Oliveira, M. B. F.; Pinto, A. V.; Santana, A. E. G.; Goulart, M. O. F.; *Acta Trop.* **2009**, *111*, 44. [Crossref]

11. Huang, Z.; Cui, Q.; Xiong, L.; Wang, Z.; Wang, K.; Zhao, Q.; Bi, F.; Wang, Q.; *J. Agric. Food Chem.* **2009**, *57*, 2447. [Crossref]

12. Sun, R.; Li, Y.; Lü, M.; Xiong, L.; Wang, Q.; *Bioorg. Med. Chem. Lett.* **2010**, *20*, 4693. [Crossref]

13. Rajanarendar, E.; Reddy, M. N.; Murthy, K. R.; Reddy, K. G.; Raju, S.; Srinivas, M.; Praveen, B.; Rao, M. S.; *Bioorg. Med. Chem. Lett.* **2010**, *20*, 6052. [Crossref]

14. Sun, R.; Li, Y.; Xiong, L.; Liu, Y.; Wang, Q.; *J. Agric. Food Chem.* **2011**, *59*, 4851. [Crossref]

15. Lima, E. P.; de Oliveira Filho, A. M.; Lima, J. W. O.; Ramos Jr., A. N.; Cavalcanti, L. P. G.; Pontes, R. J. S.; *Rev. Soc. Bras. Med. Trop.* **2006**, *39*, 259. [Crossref]

16. Neves-Filho, R. A. W.; da Silva, C. A.; da Silva, C. S. B.; Brustein, V. P.; Navarro, D. M. A. F.; dos Santos, F. A. B.; Alves, L. C.; Cavalcanti, M. G. S.; Srivastava, R. M.; Carneiro-da-Cunha, M. G.; *Chem. Pharm. Bull.* **2009**, *57*, 819. [Crossref]

17. da Silva, J. B. P.; Navarro, D. M. A. F.; da Silva, A. G.; Santos, G. K. N.; Dutra, K. A.; Moreira, D. R.; Ramos, M. N.; Espíndola, J. W. P.; de Oliveira, A. D. T.; Brondani, D. J.; Leite, A. C. L.; Hernandes, M. Z.; Pereira, V. R. A.; da Rocha, L. F.; de Castro, M. C. A. B.; de Oliveira, B. C.; Lan, Q.; Merz Jr., K. M.; *Eur. J. Med. Chem.* **2015**, *100*, 162. [Crossref]

18. Santos, S. R. L.; Silva, V. B.; Melo, M. A.; Barbosa, J. D. F.; Santos, R. L. C.; Sousa, D. P.; Cavalcanti, S. C. H.; *Vector-Borne Zoonotic Dis.* **2010**, *10*, 1049. [Crossref]

19. de Sousa, D. P.; Vieira, Y. W.; Uliana, M. P.; Melo, M. A.; Brocksom, T. J.; Cavalcanti, S. C. H.; *Parasitol. Res.* **2010**, *107*, 741. [Crossref]

20. Santos, S. R. L.; Melo, M. A.; Cardoso, A. V.; Santos, R. L. C.; de Sousa, D. P.; Cavalcanti, S. C. H.; *Chemosphere* **2011**, *84*, 150. [Crossref]

21. da Silva, J. B. P.; Hallwass, F.; da Silva, A. G.; Moreira, D. R.; Ramos, M. N.; Espíndola, J. W. P.; de Oliveira, A. D. T.;

Brondani, D. J.; Leite, A. C. L.; Merz Jr., K. M.; *J. Mol. Struct.* **2015**, *1093*, 219. [Crossref]

22. Becke, A. D.; *J. Chem. Phys.* **1993**, *98*, 5648. [Crossref]

23. Frisch, M. J.; Trucks, G. W.; Schlegel, H. B.; Scuseria, G. E.; Robb, M. A.; Cheeseman, J. R.; Scalmani, G.; Barone, V.; Mennucci, B.; Petersson, G. A.; Nakatsuji, H.; Caricato, M.; Li, X.; Hratchian, H. P.; Izmaylov, A. F.; Bloino, J.; Zheng, G.; Sonnenberg, J. L.; Hada, M.; Ehara, M.; Toyota, K.; Fukuda, R.; Hasegawa, J.; Ishida, M.; Nakajima, T.; Honda, Y.; Kitao, O.; Nakai, H.; Vreven, T.; Montgomery Jr., J. A.; Peralta, J. E.; Ogliaro, F.; Bearpark, M.; Heyd, J. J.; Brothers, E.; Kudin, K. N.; Staroverov, V. N.; Kobayashi, R.; Normand, J.; Raghavachari, K.; Rendell, A.; Burant, J. C.; Iyengar, S. S.; Tomasi, J.; Cossi, M.; Rega, N.; Millam, N. J.; Klene, M.; Knox, J. E.; Cross, J. B.; Bakken, V.; Adamo, C.; Jaramillo, J.; Gomperts, R.; Stratmann, R. E.; Yazyev, O.; Austin, A. J.; Cammi, R.; Pomelli, C.; Ochterski, J. W.; Martin, R. L.; Morokuma, K.; Zakrzewski, V. G.; Voth, G. A.; Salvador, P.; Dannenberg, J. J.; Dapprich, S.; Daniels, A. D.; Farkas, Ö.; Foresman, J. B.; Ortiz, J. V; Cioslowski, J.; Fox, D. J.; *Gaussian 09, Rev A.02*; Gaussian, Inc., Wallingford, CT, 2009.

24. Wold, S.; *Chemom. Intell. Lab. Syst.* **2001**, *58*, 83. [Crossref]

25. R Core Team; *R: A Language and Environment for Statistical Computing*, 3.6.2; R Foundation for Statistical Computing, Vienna, 2019.

26. Mevik, B.-H.; Wehrens, R.; *J. Stat. Software* **2007**, *18*, 1. [Crossref]

27. Ferreira, M. M. C.; *J. Braz. Chem. Soc.* **2002**, *13*, 742. [Crossref]

28. Berman, H.; Henrick, K.; Nakamura, H.; *Nat. Struct. Mol. Biol.* **2003**, *10*, 980. [Crossref]

29. Dyer, D. H.; Lovell, S.; Thoden, J. B.; Holden, H. M.; Rayment, I.; Lan, Q.; *J. Biol. Chem.* **2003**, *278*, 39085. [Crossref]

30. Sanner, M. F.; Huey, R.; Dallakyan, S.; Karnati, S.; Lindstrom, W.; Morris, G. M.; Norledge, B.; Omelchenko, A.; Stoffler, D.; Vareille, G.; *AutoDockTools* v1.5.2 revision 2; Molecular Graphics Laboratory, The Scripps Research Institute, USA, 2008.

31. Gasteiger, J.; Marsili, M.; *Tetrahedron* **1980**, *36*, 3219. [Crossref]

32. Morris, G. M.; Huey, R.; Lindstrom, W.; Sanner, M. F.; Belew, R. K.; Goodsell, D. S.; Olson, A. J.; *J. Comput. Chem.* **2009**, *16*, 2785. [Crossref]

33. Wallace, A. C.; Laskowsky, R. A.; Thornton, J. M.; *Protein Eng., Des. Sel.* **1995**, *8*, 127. [Crossref]

34. World Health Organization (WHO), *Guidelines for Laboratory and Field Testing of Mosquito Larvicides*; WHO: Geneva, Switzerland, 2005. [Link] accessed in August 2022

35. Navarro, D. M. A. F.; de Oliveira, P. E. S.; Potting, R. P. J.; Brito, A. C.; Fital, S. J. F.; Sant'Ana, A. E. G.; *J. Appl. Entomol.* **2003**, *127*, 46. [Crossref]

36. Bianco, E. M.; Pires, L.; Santos, G. K. N.; Dutra, K. A.; Reis, T. V. N.; Vasconcelos, E. R. T. P. P.; Cocentino, A. L. M.; Navarro, D. M. A. F.; *Ind. Crops Prod.* **2013**, *43*, 270. [Crossref]

37. Santos, G. K. N.; Dutra, K. A.; Lira, C. S.; Lima, B. N.; Napoleão, T. H.; Paiva, P. M. G.; Maranhão, C. A.; Brandão, S. S. F.; Navarro, D. M. A. F.; *Molecules* **2014**, *19*, 16573. [Crossref]

38. *StatPlus*, Pro 5 (6.7.0.3); AnalystSoft, WALNUT, CA, USA, 2007.

39. Bai, L.; Wang, J.-X.; Zhang, Y.; *Green Chem.* **2003**, *5*, 615. [Crossref]

40. Scotti, L.; Scotti, M. T.; Silva, V. B.; Santos, S. R. L.; Cavalcanti, S. C. H.; Mendonca Jr., F. J. B.; *Med. Chem.* **2014**, *10*, 201. [Crossref]

41. Kyte, J.; Doolittle, R. F.; *J. Mol. Biol.* **1982**, *157*, 105. [Crossref]

42. Guo, F.; Zhang, D.; Kahyaoglu, A.; Farid, R. S.; Jordan, F.; *Biochemistry* **1998**, *37*, 13379. [Crossref]

43. Gallagher, P. G.; Zhang, Z.; Morrow, J. S.; Forget, B. G.; *Lab. Invest.* **2004**, *84*, 229. [Crossref]

44. Steuber, H.; Heine, A.; Klebe, G.; *J. Mol. Biol.* **2007**, *368*, 618. [Crossref]

45. Singarapu, K. K.; Ahuja, A.; Potula, P. R.; *Biochemistry* **2016**, *55*, 4919. [Crossref]